Effect of Silver Doping on the Physical Properties of Zirconia Dioxide Nanostructures Thin Films

Athraa Mohammad Abdullah[1], Tariq Juma Mahmood[1], Murtada Kudhier Abbas Hassan[2], Karrar Noor Hussein[3] and Taghreed Khalid Hameed[4]

[1]*Directorate of Education Baghdad Al-Karkh 2, Ministry of Education, 10001 Baghdad, Iraq*
[2]*Department of Scientific Affairs, Mustansiriyah University, 10052 Baghdad, Iraq*
[3]*Department of Radiology, Al-Manara College for Medical Sciences, 62001 Amarah, Iraq*
[4]*Department of Physics, College of Education, Mustansiriyah University, 10052 Baghdad, Iraq*
taghreedkhalid@uomustansiriyah.edu.iq

Keywords: ZrO_2, Ag, Thin Films, CSP, XRD, AFM, Band Gap, Sensitivity, Resistance.

Abstract: Chemical spray pyrolysis (CSP) was employed to deposit ZrO_2:Ag thin films with good uniformity and adhesion. X-ray diffraction analysis confirmed the formation of a polycrystalline cubic phase, while Ag incorporation promoted grain growth and improved crystalline quality through the reduction of dislocation density and lattice strain. Atomic force microscopy (AFM) revealed a progressive decrease in surface roughness and particle size with increasing Ag content, indicating the development of a denser and more compact film morphology. Optical transmittance measurements showed moderate transparency in the range of 72.6-76.2%, with a slight decrease upon doping, although the films retained good transparency in the visible region. The optical band gap was found to narrow from 5.18 eV to 5.07 eV, which can be attributed to the introduction of localized defect states within the band structure. Gas-sensing measurements performed at 200 ppm NO_2 and an operating temperature of 130 °C demonstrated that undoped ZrO_2 films exhibited the highest sensitivity while Ag doping led to a gradual reduction in sensing performance.

1 INTRODUCTION

Zirconia thin films (ZrO_2) are classified as transition-metal oxides [1], [2] and exhibit attractive physical, optical, and chemical properties [3]-[6]. It has shown excellent hardness, very low electrical conductivity, high melting point, excellent thermodynamic stability [7], high refractive index, large dielectric constant, and a wide optical band gap [8]-[12]. It is thanks to these properties that ZrO_2 thin films have attracted tremendous interest as well as applications in other study areas like optical filtering [13], memory devices [14], and use as capacitors [15] in dynamic random-access memory [16]. Researchers have consequently looked into the creation of ZrO_2 thin films on a variety of substrates using a variety of techniques due to the vast range of essential applications. For example, pulsed laser deposition [17], the electron beam evaporation method [18], sputtering a ZrO_2 target using an argon-oxygen gas mixture at varied total gas pressures [19], sol-gel [20], RF sputtering deposition [21], and direct current magnetron sputtering technique [22]. Recently, metal element doping of zirconium dioxide thin films has been extensively investigated to improve their structural, optical, and functional properties [23], [24]. Among the diverse dopants, silver (Ag) has attracted much attention due to its remarkable electrical conductivity, catalytic properties, and strong affinity for oxygen species [25], [26]. The insertion of Ag into the ZrO_2 lattice can lead to modifications in the crystal structure, changes in the optical band gap, and an enhancement in surface activity that could be beneficial for sensing applications [27]. Ag-doped ZrO_2 thin films were created in this work using CSP) process. This study's primary goal is to examine how Ag doping affects the structural, optical, and sensing properties of ZrO_2 thin films.

2 EXPERIMENTAL

Thin ZrO_2:Ag films were deposited through the CSP technique. 0.1 M ($ZrOCl_2.8H_2O$) was dissolved in 100 milliliters of redistilled water to prepare the solution. Doping with 2% and 4% Ag was applied. 400°C was maintained as the base temperature. A spray rate of 0.2 ml/spray, a 28 cm distance from the base to the sprayer, a 9-second spray duration, an interval between subsequent sprays of 1.5 minutes, and 105 Pa of air as the transport gas were considered suitable parameters. The gravimetric measurement indicated a film thickness of about 325 ± 25 nm. XRD measured the structural features. The surface morphology was characterized using atomic force microscopy (AFM) with an SPM-AA3000 scanning probe microscope (Angstrom Advanced Inc.). Transmittance was obtained using a double-beam spectrophotometer. The gas sensing performance was assessed by measuring the variation in electrical resistance within a custom-designed cylindrical chamber (9 cm radius and 19 cm height) under controlled H_2 gas exposure conditions.

3 RESULTS AND DISCUSSION

Figure 1 presents the XRD patterns of the synthesized films, confirming the formation of a well-defined crystalline structure. The diffraction peaks observed at 24.48°, 31.42°, 49.26°, and 63.22° were indexed to the (011), (1110), (220), and (222) crystallographic planes, respectively. These diffraction peaks are consistent with the ICDD standard (File No. 37-1484), indicating the formation of a cubic phase.

The crystallite size was estimated using the Scherrer method, while the dislocation density and lattice strain were calculated according to the standard equations reported in the literature [28]–[32]. The calculated structural parameters are summarized in Table 1. The results show that increasing the Ag concentration promotes crystallite growth, with the average crystallite size increasing from 17.26 to 32.10 nm. This behavior suggests that silver doping enhances atomic diffusion and facilitates crystallite coalescence during film growth, leading to the formation of larger crystallites [22].

In contrast, both the dislocation density and lattice strain gradually decreased as the Ag concentration increased. The dislocation density decreased from 39.34 to 24.38, while the lattice strain decreased from 27.58 to 20.08. These changes indicate an improvement in the crystalline quality of the films, as lower dislocation density and lattice strain are associated with fewer lattice defects and reduced internal stresses within the crystal structure [15], [16]. The variation of FWHM, crystallite size, dislocation density, and lattice strain with Ag concentration is presented in Figure 2.

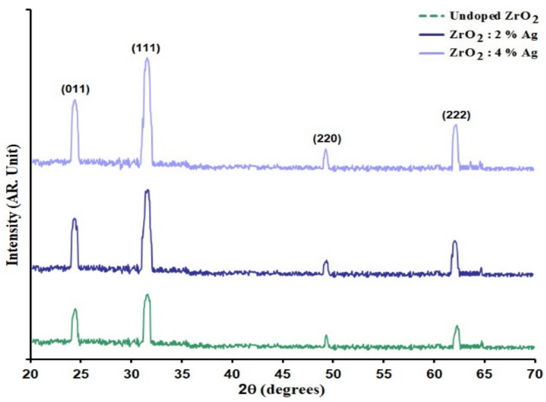

Figure 1: XRD patterns of undoped and Ag-doped ZrO_2 thin films.

Table 1: Structural parameters and optical band gap of undoped and Ag-doped ZrO_2 thin films.

Sample	(hkl) Plane	2 θ (°)	FWHM (°)	E_g (eV)	D (nm)	$\delta \times 10^{14}$ (lines/m^2)	$\varepsilon \times 10^{-4}$
Undoped ZrO_2	100	31.42	0.48	5.18	17.26	39.34	27.58
ZrO_2: 2% Ag	100	31.38	0.44	5.13	29.32	27.21	24.82
ZrO_2: 4% Ag	100	31.33	0.40	5.08	32.10	24.38	20.08

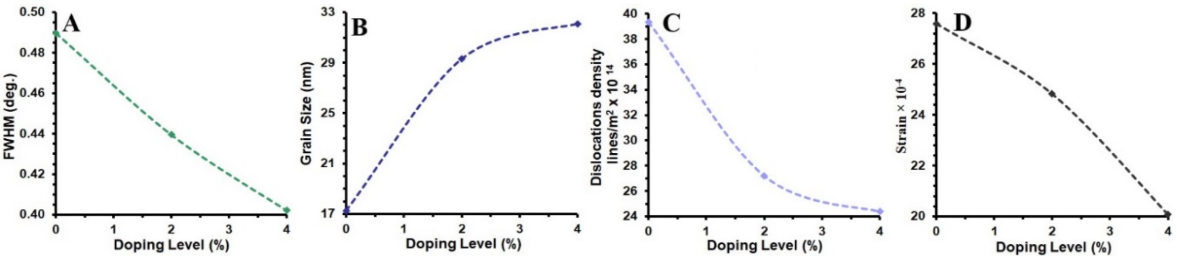

Figure 2: Structural parameters of undoped and Ag-doped ZrO_2 thin films: a) FWHM, b) crystallite size, c) dislocation density, and d) lattice strain as a function of Ag concentration.

Atomic force microscopy (AFM) was employed to investigate the surface morphology of pure and Ag-doped ZrO_2 thin films. The AFM images presented in Figure 3 reveal a homogeneous granular morphology with nanostructured grains uniformly distributed over the film surface. Surface characteristics were evaluated in terms of average particle size (Pav), average roughness (Ra), and root-mean-square roughness (RMS), and the corresponding values are summarized in Table 2.

Table 2: AFM parameters of ZrO_2: Ag films.

Specimen	P_{av} nm	Ra (nm)	RMS (nm)
undoped ZrO_2	78.6	6.35	7.92
ZrO_2: 2% Ag	54.1	4.16	6.16
ZrO_2: 4% Ag	41.4	3.08	3.28

The results demonstrate that Ag incorporation significantly modifies the surface morphology of the films. The average particle size decreased from 78.6 nm for undoped ZrO_2 to 54.1 nm and 41.4 nm for the films doped with 2 and 4% Ag, respectively. Likewise, the average roughness (Ra) decreased from 6.35 to 4.16 and 3.08 nm, while the RMS roughness decreased from 7.92 to 6.16 and 3.28 nm. These results indicate that Ag doping suppresses grain growth and promotes the formation of a smoother and more compact film surface, most likely by increasing the density of nucleation sites during film growth [33].

The optical transmittance spectra of the deposited films are shown in Figure 4. All samples exhibit relatively high transparency in the visible region, with transmittance values ranging from approximately 72.6% to 76.2%. The transmittance gradually increases with wavelength, reflecting reduced optical absorption at lower photon energies. This behavior is attributed to the insufficient photon energy required to excite electrons from the valence band to the conduction band or to defect-related energy levels [34].

The absorbance spectra shown in Figure 5 were calculated from the measured transmittance using the standard optical relationship [35]. The undoped ZrO_2 film exhibits the lowest absorbance, whereas the absorbance increases progressively with increasing Ag concentration. This enhancement is attributed to the incorporation of Ag into the ZrO_2 lattice, which introduces additional impurity and defect states within the band gap, thereby increasing the probability of electronic transitions and photon absorption [36], [37].

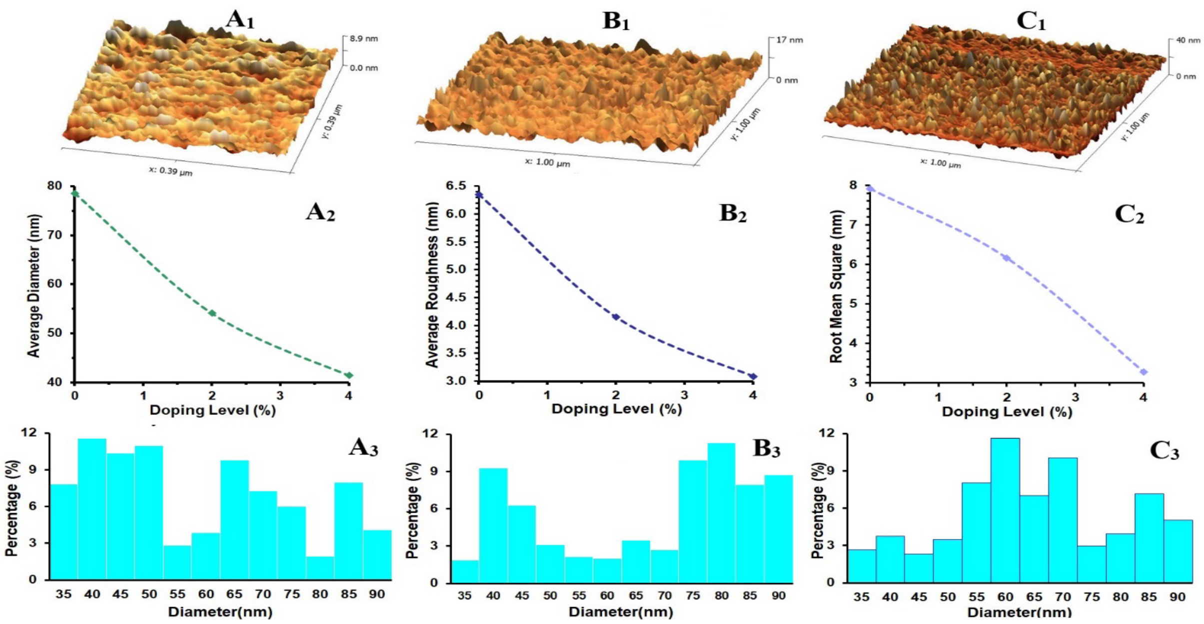

Figure 3: AFM surface morphology of undoped and Ag-doped ZrO_2 thin films.

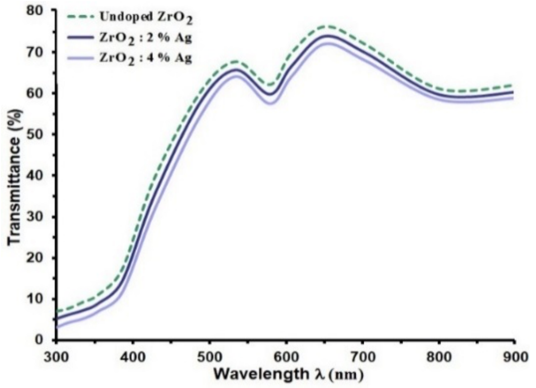

Figure 4: Optical transmittance spectra of undoped and Ag-doped ZrO_2 thin films.

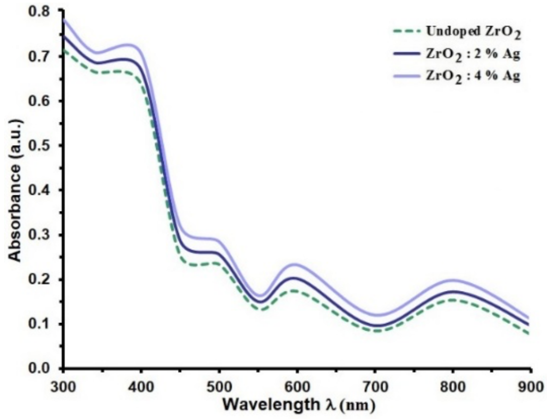

Figure 5: Optical absorbance spectra of undoped and Ag-doped ZrO_2 thin films.

The absorption coefficient was calculated from the absorbance spectra using the conventional relationship for thin films [38]. As shown in Figure 6, the absorption coefficient increases with Ag concentration, particularly near the absorption edge, indicating enhanced optical absorption. The obtained values exceed 10^4 cm^{-1}, confirming strong optical absorption and the predominance of direct electronic transitions. This enhancement is attributed to Ag-induced modifications in the electronic structure, which introduce additional localized states that facilitate photon absorption and electronic excitation [39], [40].

The optical band gap was determined using the Tauc method for direct electronic transitions [41]. Figure 7 shows that the optical band gap decreases progressively with increasing Ag concentration, from 5.18 eV for undoped ZrO_2 to approximately 5.07 eV for the film containing the highest Ag content. This reduction is attributed to the formation of impurity and defect states associated with Ag incorporation into the ZrO_2 lattice. These localized energy levels narrow the effective band gap by facilitating electronic transitions at lower photon energies. In addition, Ag doping increases structural disorder, resulting in band-tail formation and a slight reduction in the optical band gap [42], [43].

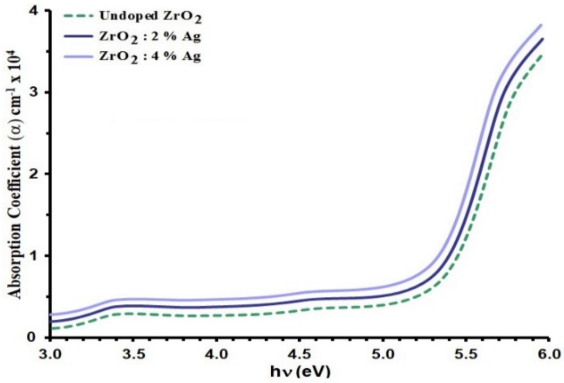

Figure 6: Absorption coefficient as a function of photon energy for undoped and Ag-doped ZrO_2 thin films.

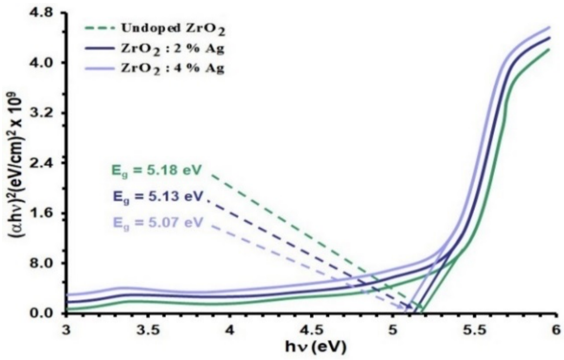

Figure 7. Tauc plots for determining the direct optical band gap of undoped and Ag-doped ZrO_2 thin films.

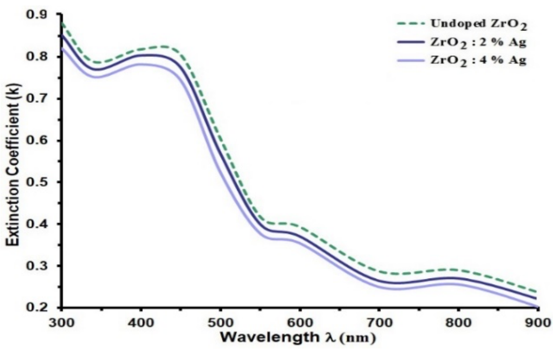

Figure 8: Extinction coefficient as a function of wavelength for undoped and Ag-doped ZrO_2 thin films.

The extinction coefficient was calculated from the optical absorption data using the standard relationship [44]. As illustrated in Figure 8, the extinction coefficient increases rapidly in the ultraviolet region and gradually decreases with increasing wavelength. The nonzero values observed below the fundamental absorption edge indicate the presence of sub-band-gap absorption, which is commonly associated with structural defects, impurity levels, and localized electronic states introduced during film growth and Ag incorporation [45].

The refractive index was determined from the optical reflectance data using the conventional model described in the literature [46,47]. Figure 9 shows that the refractive index exhibits normal optical dispersion, increasing gradually with wavelength for all samples. However, the refractive index decreases with increasing Ag concentration, indicating that Ag incorporation modifies the electronic polarizability and microstructure of the ZrO_2 films, thereby reducing their optical density [48], [49].

The gas-sensing performance of the films was evaluated at an operating temperature of 130 °C using 200 ppm NO_2 gas. The resistance responses presented in Figure 10 show that the undoped ZrO_2 film exhibits the lowest electrical resistance, indicating more efficient interaction with NO_2 molecules and higher charge-carrier mobility. In contrast, the film containing 4% Ag exhibits the highest resistance, suggesting that Ag incorporation modifies the electronic structure and limits charge transport during gas adsorption [50], [51].

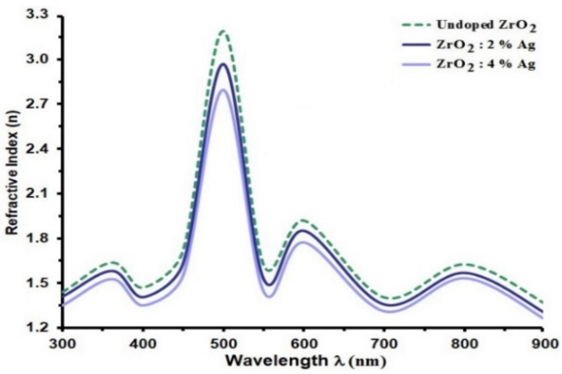

Figure 9: Refractive index as a function of wavelength for undoped and Ag-doped ZrO_2 thin films.

The sensor sensitivity was calculated using the standard resistance-based expression [52]. Figure 11 demonstrates that the sensitivity decreases with increasing Ag concentration over the investigated NO_2 concentration range. At 110, 160, and 210 ppm NO_2, the sensitivity decreases from 31.16% for undoped ZrO_2 to 6.76%, 32.29% to 7.95%, and 34.18% to 9.08%, respectively, for the films containing 2% and 4% Ag. This behavior indicates that excessive Ag incorporation reduces the gas-sensing response, most likely because dopant-induced structural and electronic modifications suppress charge-carrier transport and decrease the number of active adsorption sites available for NO_2 molecules [53]–[58].

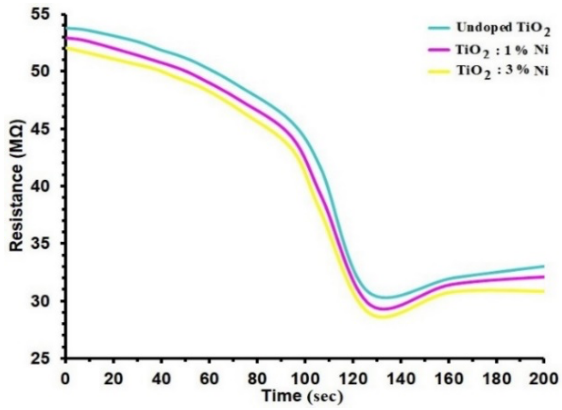

Figure 10: Dynamic resistance response of undoped and Ag-doped ZrO_2 thin films toward 200 ppm NO_2 at an operating temperature of 130 °C.

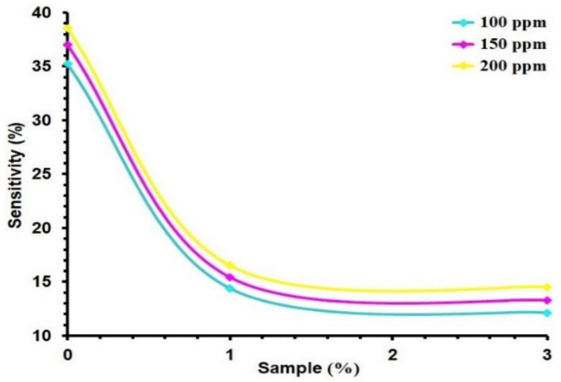

Figure 11: NO_2 gas sensitivity of undoped and Ag-doped ZrO_2 thin films at different gas concentrations.

4 CONCLUSIONS

In summary, Ag-doped ZrO_2 thin films were successfully deposited using the chemical spray pyrolysis (CSP) technique, demonstrating good reproducibility and uniform coverage. Structural characterization confirmed that the incorporation of Ag ions promotes crystallite growth, improves the film matrix. Additionally, surface morphology analysis revealed a smoother and more homogeneous surface with increasing Ag concentration, accompanied by a noticeable reduction in average particle size (from AFM) and surface roughness, even though the average crystallite (grain) size determined from XRD increased with Ag content. Optical investigations indicated that all films maintained high transparency in the visible region, while the optical band gap decreased systematically from 5.18 eV to 5.08 eV with Ag doping, likely due to the introduction of localized energy states within the band structure. Despite these improvements, gas-sensing measurements toward NO_2 demonstrated that undoped ZrO_2 films exhibited the highest sensitivity, whereas Ag incorporation led to a gradual decline in sensing performance. This reduction may be attributed to altered charge transport mechanisms and reduced active adsorption sites. Therefore, optimizing dopant concentration is essential for balancing material properties and achieving application-specific performance.

ACKNOWLEDGMENTS

This research was financially supported by Mustansiriyah University (www.uomustansiriyah.edu.iq) through its institutional academic research program.

REFERENCES

[1] P. Chandramohan, R. R. Varshaa, S. Biswas, A. L. Rufus, and T. K. Mohan, "Phase stability and evaluation of crystal structure of transition metal substituted zirconium oxide," Ceramics International, 2025.

[2] D. Bouras, M. Fellah, R. Barille, M. Zerouali, N. Hambli, and G. A. El-Hiti, "Comparative study of zirconium-zinc oxide thin films on ceramic and glass substrates: Structural, optical, and photocatalytic properties," Inorganic Chemistry Communications, vol. 171, article no. 113561, 2025.

[3] N. Yavuzkanat and T. Şahmaran, "Radiation Shielding and Physical Properties of ZrO_2-Modified Borosilicate Glasses: A Monte Carlo, Theoretical, and AI-Based Study," Radiation Physics and Chemistry, article no. 113698, 2026.

[4] V. R. Kumar, K. K. Kumar, L. Vijayalakshmi, J. Lim, V. R. Kumar, and N. Veeariah, "Optimized reddish-orange emission in Pr^{3+} ions doped Pb_3O_4-ZrO_2-B_2O_3-SiO_2 glasses for advanced photonic applications," Journal of Non-Crystalline Solids, vol. 673, article no. 123878, 2026.

[5] R. Vidrio, Y. Tong, J. Liu, B. Schneider, W. O. Nachlas, N. Curtis, and J. T. Choy, "Mapping optical, chemical, structural features in ZrO_2 via cross-sectional SEM-Cathodoluminescence correlation microscopy," arXiv preprint, arXiv:2601.19428, 2026.

[6] R. Manimaran, S. Pramanik, and S. Roy, "A Combined Effect of Calcium Silicate and Silver on the Prediction of Mechanical Properties of 3 mol% Yttria-stabilized Zirconia Matrix-based Hybrid Ceramic Composites via TOPSIS," Ceramics International, 2026.

[7] V. Subramaniyam, N. Eswaramoorthy, and J. Balasundaram, "Current status and outlook of Zr, ZrO_2, and ZrS_2 quantum dots: a review," Chemical Papers, pp. 1-28, 2026.

[8] A. Alruwaili, M. O. Alziyadi, M. J. Alawi, and M. S. Shalaby, "Tuning structural, dielectric constants, optoelectrical parameters, and linear/nonlinear optical features of PVC/ZrO_2 nanocomposite films for flexible electronic devices," Journal of Inorganic and Organometallic Polymers and Materials, vol. 35, no. 5, pp. 3786-3801, 2025.

[9] S. Alattar, M. Nadafan, and M. Khashehchi, "Exploring the impact of thin film thicknesses on the linear and nonlinear optical properties of ZrO_2 thin film," Journal of Optics, pp. 1-10, 2024.

[10] S. Ram and G. P. Singh, "Advanced ZrO_2-Based Ceramic Nanocomposites for Optical and Other Engineering Applications," in Composite Materials: Processing, Applications, Characterizations. Berlin, Heidelberg: Springer Berlin Heidelberg, pp. 497-570, 2016.

[11] E. S. R. Khattab, S. S. Abd El Rehim, W. M. Hassan, and T. S. El-Shazly, "Band structure engineering and optical properties of pristine and doped monoclinic zirconia (m-ZrO_2): density functional theory theoretical prospective," ACS Omega, vol. 6, no. 44, pp. 30061-30068, 2021.

[12] P. Carvalho, J. Borges, M. S. Rodrigues, N. P. Barradas, E. Alves, J. P. Espinós, and F. Vaz, "Optical properties of zirconium oxynitride films: The effect of composition, electronic and crystalline structures," Applied Surface Science, vol. 358, pp. 660-669, 2015.

[13] V. Chauhana, D. Guptaa, S. Upadhyayc, J. Ramd, S. Kumare, and R. Kumara, "Advancement of high-k ZrO_2 for potential applications: a review," Indian Journal of Pure & Applied Physics, vol. 59, no. 12, pp. 811-826, 2021.

[14] P. D. Lomenzo, S. Li, L. Pintilie, C. M. Istrate, T. Mikolajick, and U. Schroeder, "Memory Window Enhancement in Antiferroelectric RAM by Hf Doping in ZrO_2," IEEE Electron Device Letters, vol. 43, no. 9, pp. 1447-1450, 2022.

[15] H. An, W. Lee, S. H. Kim, C. J. Cho, D. G. Kim, D. S. Kwon, and C. S. Hwang, "Controlling the electrical characteristics of ZrO_2/Al_2O_3/ZrO_2 capacitors by adopting a Ru top electrode grown via atomic layer deposition," Physica Status Solidi (RRL) - Rapid Research Letters, vol. 13, no. 3, article no. 1800454, 2019.

[16] Y. U. Ryu, H. Oh, I. Hwang, Y. Park, Y. Kim, and W. Jeon, "Leakage current control of Y-HfO_2 for dynamic random access memory applications via ZrO_2 stacking," Ceramics International, vol. 50, no. 21, pp. 41483-41489, 2024.

[17] H. Irhayyim and S. A. Hussain, "Structural and optical properties of pure and AgNPs doped ZrO_2 thin films prepared by pulse laser deposition method," in AIP Conference Proceedings, vol. 2845, no. 1, p. 070030, 2023.

[18] R. Shakoury, N. Talebani, A. Zelati, Ș. Ţălu, A. Arman, S. Mirzaei, and A. Jafari, "The effect of thickness and film homogeneity on the optical and microstructures of the ZrO_2 thin films prepared by electron beam evaporation method," Optical and Quantum Electronics, vol. 53, no. 8, p. 441, 2021.

[19] Houska, J. Rezek, and R. Cerstvy, "Dependence of the ZrO_2 growth on the crystal orientation: Growth simulations and magnetron sputtering," Applied Surface Science, vol. 572, article no. 151422, 2022.

[20] G. Shishodia, S. Gupta, N. Pahwa, and P. K. Shishodia, "ZrO_2 nanoparticles synthesized by the sol-gel method: Dependence of size on pH and annealing temperature," Journal of Electronic Materials, vol. 53, no. 9, pp. 5159-5168, 2024.

[21] R. Shakoury, A. Arman, S. Miri, M. Mardani, S. Rezaee, A. Boochani, and K. Sherafat, "Optical properties and microstructure of ZrO_2 thin films deposited by RF magnetron sputtering: case study on effects of different working temperatures," Optical and Quantum Electronics, vol. 54, no. 11, p. 682, 2022.

[22] H. Zegtouf, N. Saoula, M. Azibi, L. Bait, N. Madaoui, M. R. Khelladi, and M. Kechouane, "A study of properties of ZrO_2 thin films deposited by magnetron sputtering under different plasma parameters: Biomedical application," Journal of Electrical Engineering, vol. 70, no. 7, pp. 117-121, 2019.

[23] A. U. R. Khan, M. Ramzan, M. Imran, M. Zubair, S. Shahab, S. J. Ahmed, and M. F. Iqbal, "Tailoring the structural, optical and electrical properties of zinc oxide nanostructures by zirconium doping," Coatings, vol. 13, no. 1, p. 34, 2022.

[24] M. Bolbol, O. H. Abd-Elkader, H. Elshimy, Z. I. Zaki, S. A. Shata, M. Kamel, and N. Y. Mostafa, "The effect of Zr(IV) doping on TiO_2 thin film structure and optical characteristics," Results in Physics, vol. 42, article no. 105955, 2022.

[25] M. Assis, A. C. M. Renno, J. Andres, and E. Longo, "Defect engineering in silver-based bimetallic semiconductors: recent advances and future perspective," ACS Omega, vol. 10, no. 22, pp. 22323-22346, 2025.

[26] F. Nasim, H. Malik, G. Xu, H. Dong, and M. A. Nadeem, "Exploring the heterointerface of silver nanoparticles and cobalt oxide nanorings toward the oxygen reduction reaction," Journal of Materials Chemistry A, vol. 13, no. 29, pp. 23981-23997, 2025.

[27] Y. Yan, G. Turdi, A. Yimit, and P. Nizamidin, "Ag-doped $ZnFe_2O_4$ nanoparticles for highly selective room-temperature H_2S detection: Experiment and DFT study," Materials Science in Semiconductor Processing, vol. 208, article no. 110495, 2026.

[28] R. S. Ali, M. K. Mohammed, A. A. Khadayeir, Z. M. Abood, N. F. Habubi, and S. S. Chiad, "Structural and optical characterization of sprayed nanostructured indium doped Fe_2O_3 thin films," Journal of Physics: Conference Series, vol. 1664, no. 1, article no. 012016, 2016.

[29] M. A. Issa and K. A. Aadim, "Optical and structural characterization of ZnO:NiO nano composite prepared by pulsed laser deposition method," J. Opt., vol. 54, pp. 2357-2362, 2025.

[30] F. S. Ahmed, N. Y. Ahmed, R. S. Ali, N. F. Habubi, K. H. Abass, and S. S. Chiad, "Effects of substrate type on some optical and dispersion properties of sprayed CdO thin films," NeuroQuantology, vol. 18, no. 3, pp. 56-65, 2020.

[31] A. Ibrahem, A. M. A. Karim, and T. H. Mubarak, "Study of the effect of cobalt on the structural properties of nickel ferrite prepared by chemical co-precipitation thermal method," Materials Today Proceedings, 2023.

[32] S. S. Chiad, K. H. Abass, T. H. Mubarak, N. F. Habubi, M. K. Mohammed, and A. A. Khadayeir, "Fabrication and study the structure, optical and dispersion parameters of PMMA with $InCl_3$ additive," Journal of Global Pharma Technology, vol. 11, no. 4, pp. 369-375, 2019.

[33] Giorio, G. Maculotti, F. Gattucci, G. Genta, C. Balagna, and M. Galetto, "Topographical and mechanical properties of sputtered composite coatings with silver nanoparticles for functional surfaces," Materials Today Communications, article no. 114894, 2026.

[34] A. Issa and K. A. Aadim, "Influence of Laser Energy On Structural and Optical Properties of ZnO(x):NiO(1−x) Films Prepared by Pulse Laser Deposition," J. Opt., 2024.

[35] H. T. Salloom, E. H. Hadi, N. F. Habubi, S. S. Chiad, M. Jadan, and J. S. Addasi, "Characterization of silver content upon properties of nanostructured nickel oxide thin films," Digest Journal of Nanomaterials and Biostructures, vol. 15, no. 4, pp. 1189-1195, 2020.

[36] R. Kaliyaperumal, K. Nagaraj, V. K. Poovan, K. Sakthikumar, C. Govindasamy, and A. S. Sivakumar, "Hydrothermal implementation with Zirconia: synthesis, characterization and investigation of biocidal activity of Ag/ZrO_2 nanocomposites," Zeitschrift für Physikalische Chemie, vol. 238, no. 2, pp. 209-221, 2024.

[37] A. J. Mawat, M. H. Al-Timimi, W. H. Albanda, and M. Z. Abdullah, "Morphological and optical properties of Mg_{1}-xCdSx nanostructured thin films," AIP Conference Proceedings, vol. 2475, article no. 090019, 2023.

[38] A. Issa and K. A. Aadim, "Study the structural and optical properties of Zinc Oxide prepared by pulse laser deposition," J. Opt., 2024.

[39] Kumar and G. B. Reddy, "Stability-inspired entrapment of Ag nanoparticles in ZrO_2 thin films," Plasmonics, vol. 11, no. 1, pp. 261-267, 2016.

[40] I. Ramadhan, A. M. Sari, K. Saptaji, I. B. Rahardja, E. Umar, S. Y. Perdana, and W. H. Azmi, "Characterization and Stability of ZrO_2-SiO_2 Nanofluids from Local Minerals Indonesia as Green Nanofluids to Application Radiator Cooling System," J. Adv. Res. Fluid Mech. Therm. Sci., vol. 111, no. 2, pp. 126-140, 2023.

[41] F. S. Ahmed, N. Y. Ahmed, R. S. Ali, N. F. Habubi, K. H. Abass, and S. S. Chiad, "Effects of substrate type on some optical and dispersion properties of sprayed CdO thin films," NeuroQuantology, vol. 18, no. 3, pp. 56-65, 2020.

[42] H. Alfannakh and B. Souayeh, "Computational assessment of ZrO_2-Al_2O_3/EG and ZrO_2-Al_2O_3-Cu/EG nanomaterial on Blasius-Rayleigh-Stokes flow influenced by an aligned magnetic field," Processes, vol. 11, no. 10, p. 2860, 2023.

[43] X. Wang, H. Cheng, Y. Min, X. Li, L. You, and J. Li, "Fe_3O_4@m-ZrO_2@Ag ternary magnetic nanocomposites for sensitive SERS sensing and photocatalytic removal of Cr(VI) and organic dyes," Composites Part B: Engineering, vol. 239, article no. 109959, 2022.

[44] A. Kasikov and L. Aarik, "Calculating the Absorption Edge of Thin Films," Bulgarian Journal of Physics, vol. 51, no. 4, 2024.

[45] M. Alrahili, "Beyond extinction efficiencies to molar extinction coefficient of silver nanoparticles," Russian Journal of Physical Chemistry B, vol. 18, no. 1, pp. 343-356, 2024.

[46] S. S. Chiad, K. H. Abass, T. H. Mubarak, N. F. Habubi, M. K. Mohammed, and A. A. Khadayeir, "Fabrication and study the structure, optical and dispersion parameters of PMMA with $InCl_3$ additive," Journal of Global Pharma Technology, vol. 11, no. 4, pp. 369-375, 2019.

[47] J. Traciak, J. Sobczak, J. P. Vallejo, L. Lugo, J. Fal, and G. Żyła, "Experimental study on the density, surface tension and electrical properties of ZrO_2-EG nanofluids," Physics and Chemistry of Liquids, vol. 61, no. 1, pp. 14-24, 2023.

[48] G. I. Waterhouse, W. T. Chen, A. Chan, and D. Sun-Waterhouse, "Achieving color and function with structure: optical and catalytic support properties of ZrO_2 inverse opal thin films," ACS Omega, vol. 3, no. 8, pp. 9658-9674, 2018.

[49] M. Kumar and G. B. Reddy, "Tailoring surface plasmon resonance in Ag: ZrO_2 nanocomposite thin films," Physica E: Low-dimensional Systems and Nanostructures, vol. 43, no. 1, pp. 470-474, 2010.

[50] M. Kumar, C. S. Sandeep, G. Kumar, Y. K. Mishra, R. Philip, and G. B. Reddy, "Plasmonic and nonlinear optical absorption properties of Ag: ZrO_2 nanocomposite thin films," Plasmonics, vol. 9, no. 1, pp. 129-136, 2014.

[51] S. S. Chiad, H. A. Noor, O. M. Abdulmunem, N. F. Habubi, M. Jadan, and J. S. Addasi, "Optical and structural performance of nanostructured Te thin films by (CSP) with various thicknesses," Journal of Ovonic Research, vol. 16, no. 1, pp. 35-40, 2020.

[52] S. S. Chiad and T. H. Mubarak, "The effect of Ti on physical properties of Fe_2O_3 thin films for gas sensor applications," International Journal of Nanoelectronics and Materials, vol. 13, no. 2, pp. 221-232, 2020.

[53] Y. Doohee, A. Azarian, and M. R. Mozaffari, "Temporal Sculpting of Laser Pulses for Functional Engineering of Al_2O_3/AgO Films: From Structural Control to Enhanced Gas Sensing Performance," Sensors, vol. 25, no. 18, p. 5836, 2025.

[54] M. Chelly, D. Morganti, G. M. Abdullah, A. Tariq, G. Neri, E. Fazio, and C. Corsaro, "Optimization of ZrO_2-based electrode materials for simultaneous electrochemical sensing of dopamine, uric acid and tyrosine," Materials Today Communications, vol. 45, article no. 112254, 2025.

[55] J. Qian, H. Fan, S. Wang, W. Zhou, Y. Ren, C. Chen, and J. Fu, "Inverse ZrO_2/Co Catalyst Enables Robust and Efficient Glucose Hydrogenation," Green Chemistry, 2026.

[56] Wang, B. Song, and Z. Zeng, "Excellent selector performance in engineered Ag/ZrO_2:Ag/Pt structure for high-density bipolar RRAM applications," AIP Advances, vol. 7, no. 12, 2017.

[57] H. Wang, C. Gao, K. Sun, C. Shi, and X. Yan, "Highly improved performance in Ag-doped BSA films by inserting the ZrO_2 layer for nonvolatile resistive switching memory," IEEE Transactions on Electron Devices, vol. 68, no. 2, pp. 510-515, 2020.

[58] H. Bandarenka, A. Burko, D. Laputsko, L. Dronina, N. Kovalchuk, A. Podelinska, and D. Bocharov, "Ultraviolet exposure improves SERS activity of graphene-coated Ag/ZrO_2 substrates," Crystals, vol. 13, no. 11, p. 1570, 2023.